

## Size Effect in Centrifuge Cone Penetration Tests

Lech Bałachowski

Civil and Environmental Engineering Faculty, Gdańsk University of Technology,  
ul. Narutowicza 11/12, 80-952 Gdańsk, Poland, e-mail: abal@pg.gda.pl

(Received November 23, 2006; revised October 15, 2007)

### Abstract

In-flight penetration tests with 12 mm mini-cone, were performed in the centrifuge of L.C.P.C. in Nantes, in two uniform quartz sands of different grain size. Stress level effect and particle size effect on the cone resistance were analyzed. Geometry and particle size effects were found for cone penetration in coarse sand especially at a penetration less than the critical depth. The irregularities on the profile of the mini-cone penetration in coarse sand can be attributed to the particle size effect. The evidence of the geometry size effect was not very marked for the relatively narrow range of accelerations applied.

**Key words:** centrifuge, CPT, quartz sands, grain size

### 1. Introduction

An advantage of physical modelling in the centrifuge is the possibility of maintaining the same stress and strain levels between a model and a prototype. When the same soil is used for the model and the prototype, the soil behaviour can be properly modelled including barotropy effect. The centrifuge test is most relevant in modelling in the case where the effect of shear band is not dominant (Tatsuoka et al 1991). A possible distortion in the similitude conditions arises if a localization of deformations appears in the soil mass, or a shear band forms in the soil-structure interface. If the same model sand is used, the thickness of the shear band is the same for different size models and finally is also equal for the prototype to be modelled. The shear band thickness, a function of the mean grain diameter, cannot be properly scaled in physical modelling in centrifuge. Let us consider a granular media in dense state, where an important dilatancy within shear bands is expected, resulting in increased shear resistance. Due to progressive failure and the dilatancy in the shear band, a given soil in the centrifuge may be less vulnerable to post-peak softening on shear bands in a small model with reduced displacements (Bolton and Lau 1988). The smaller the model is, the larger contribution of dilatancy in the shear bands to the bearing capacity of the foundation is observed. When different size models are tested in the same soil, the particle size effect can appear. The smaller

the ratio size of the model to the average particle diameter is, the higher values of shaft friction, point resistance or bearing capacity of foundation are measured in dilative soil in centrifuge.

The recent development in centrifuge technology, including in-flight penetration tests (Gui and Bolton 1998), mini-pressurimeter tests (Dano et al 2005) and small models (Kusakabe et al 1991, Tatsuoka et al 1991, de Nicola and Randolph 1999, Lehane et al 2005), where the size of the model is getting closer to the mean grain size, needs an eventual grain size effect to be verified. The problem is relevant to all model tests, where small size models are used. The correct interpretation of such tests needs some correction factors to be applied.

## 2. Grain Size Effect

The grain size effect for shallow foundations was studied in centrifuge tests by Habib (1985), Kimura et al (1985), Tatsuoka et al (1991). According to Habib (1985), the size of the model should exceed 200 times the average grain diameter  $d_{50}$  to avoid grain size effect for slopes and retaining walls, under a small stress level. An important grain size effect was also found in centrifuge modelling of collapse of cavities in sand (Kutter et al 1994) and localization development (Stone and Wood 1992, White et al 1994). In case of a shallow foundation, when a higher stress level should be expected, Corté (1989) suggests the size of the model to be larger than 50 the average grain diameter  $d_{50}$  to avoid the grain size effect.

A significant grain size effect in the shaft friction measured on model piles can be expected due to shear band formation along the pile shaft (Boulon and Foray 1986, Chow 1997, Fioravante 2002, Lehane et al 2005, Lehane and White 2005). A series of centrifuge tests using four instrumented model piles of different diameter and two quartz sands were performed in order to study the grain size effect in shaft friction (Bałachowski 1995, Foray et al 1998). Similar test series with different diameter models were also executed by Garnier (1997) and Garnier and König (1998). In order to minimize the grain size effect during friction mobilization in rough interface and very dense sand, the diameter of the model  $B$  should exceed 160 average grain diameters  $d_{50}$  (Bałachowski 1995, Foray et al 1998). For a smooth interface no evident grain size effect was found (Reddy et al 2000). The grain size effect in shaft friction, function of soil dilatancy within the interface, decreases with the stress level. For a given interface roughness, this effect becomes important at high soil density. The interface behaviour can be modelled using the interface direct shear test with constant normal stiffness (CNS), (Wernick 1977). The particle size effect will increase the shaft friction in dilative interface (Boulon and Foray 1986), or will decrease in case of contractive interface, as given in a series of CNS tests in loose or carbonated sands (Bałachowski 2006).



The grain size effect can also appear in case of deep foundations for penetration tests in centrifuge, off-shore soil investigation or other in-situ tests using the miniaturized cones. This effect, related to the soil dilatancy, should, however be smaller than for shallow foundations or interface tests due to high stress level under the cone. Moreover, an increased soil compressibility and grain crushing, expected under the cone tip, will reduce the amount of grain size effect. For a standard CPT test the ratio size of the probe to the average grain diameter is generally large enough to ensure that the soil mass can be considered as continuum and no significant grain size effect is observed. Statistical comparison of in-situ tests with a standard 10 cm<sup>2</sup> cone and a mini-cone 1.27 cm<sup>2</sup> has shown 15% smaller cone resistance for the latter (de Lima and Tumay 1991). For the cone resistance at large depths, no particle size effect was reported in centrifuge tests in dense sand for the ratio cone diameter/average grain size ( $B/d_{50}$ ) ranging from 28 to 90 (Bolton et al 1999).

The study of the grain size effect for deep foundations was realized with a series of mini-cone penetration tests executed in a centrifuge (Gui and Bolton 1998). The tests were carried out in very dense Leighton Buzzard sand of different granulometry (in fine sand  $d_{50} = 0.225$  mm, medium sand  $d_{50} = 0.4$  mm and coarse sand  $d_{50} = 0.9$  mm). Three different size mini-cones were used (19.05 mm, 10 mm and 6.35 mm). The tests were performed according to the procedure of “modelling of models” (see Chapter 4.1) with the prototype cone 0.4 m in diameter to be modelled. The tests were interpreted in terms of the normalized cone resistance  $Q$ , defined (Lunne et al 1997) as:

$$Q = \frac{q_c - \sigma'_v}{\sigma'_v}, \quad (1)$$

where:

- $q_c$  – cone resistance,
- $\sigma'_v$  – vertical effective stress.

The normalized cone resistance is plotted (Fig. 1) against the normalized penetration depth ( $z/B$ ) (Bolton et al 1999). In case of Leighton Buzzard fine sand, no particle size effect is found (Gui and Bolton 1998). For medium and coarse sands, some extra cone resistance due to the scale effect was found when ( $B/d_{50}$ ) falls below 20. The largest scale effect related to particle size is observed in coarse sand and for the smallest cone 6.35 mm in diameter, i.e. for  $B/d_{50} = 7$ .



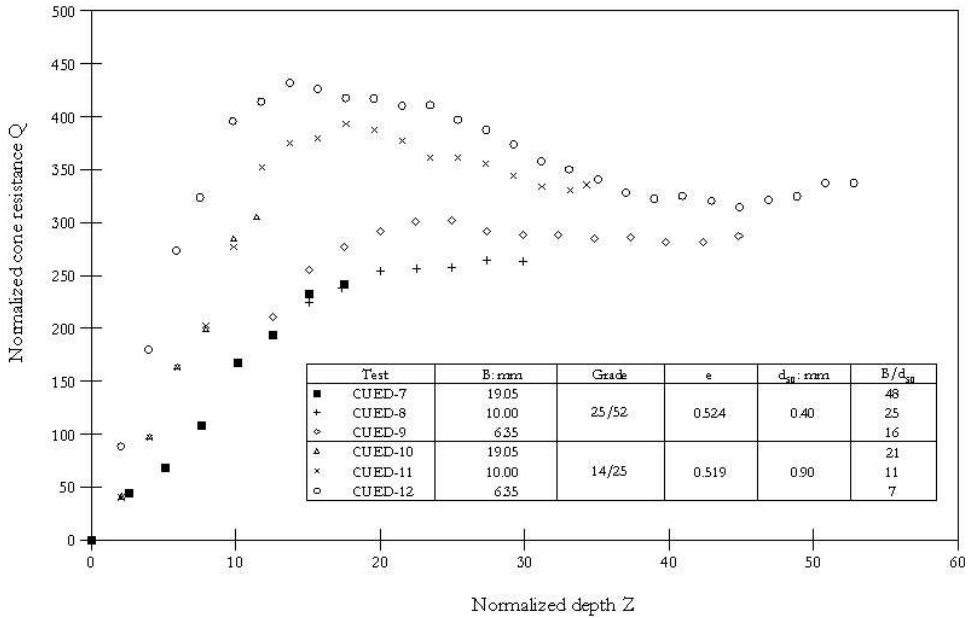


Fig. 1. Grain size effect in Leighton Buzzard sand; medium and coarse (Bolton et al 1999)

### 3. Continuous Cone Penetration

The study of the piles pushed-in from the ground surface (Kérisel 1962) shows that smaller penetration  $z$  is necessary to reach the critical depth in the case of a small diameter pile (Fig. 2).

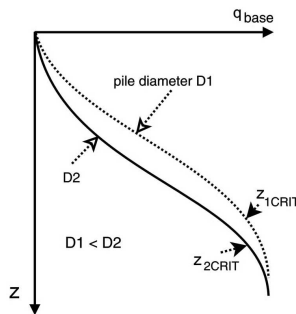


Fig. 2. Critical depth in the penetration of different diameter piles

A steady increase of cone resistance is also observed for the penetration higher than the critical depth, even at high vertical stress level. It is consistent with the CPT calibration chamber tests (Fig. 3) and the propositions of Jamiolkowski et al (1988), Jamiolkowski et al (2001).

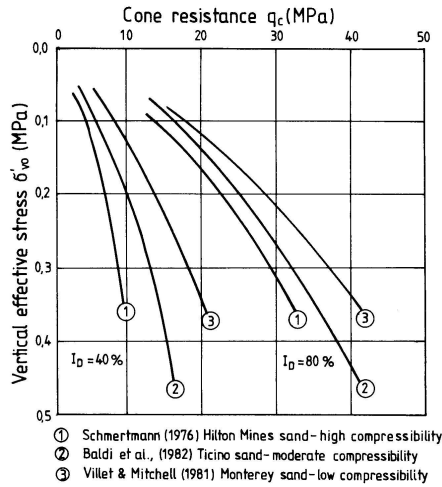


Fig. 3. Cone resistance in siliceous sands from calibration chamber tests (Lunne et al 1997)

Calibration chamber tests (Jamiolkowski et al 1988, Jamiolkowski et al 2001) have shown that under the critical depth the ratio of cone resistance to square root of the vertical effective stress is nearly constant:

$$k = \frac{q_c}{\sqrt{\sigma'_v}} \approx \text{const.} \quad (2)$$

Idealized scheme for penetration resistance is presented in Fig. 4. According to Jamiolkowski et al (2001), the density index of siliceous normally consolidated sands can be presented as:

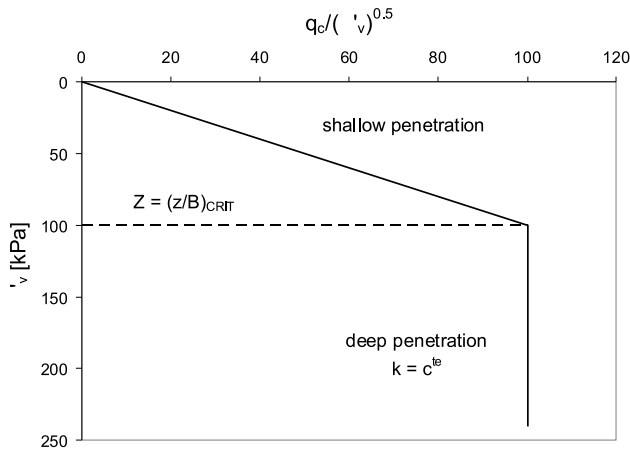


Fig. 4. Idealized penetration resistance scheme



$$I_D = \frac{1}{C_1} \ln \left( \frac{q_c}{C_0 \sqrt{\sigma'_{v0}}} \right), \quad (3)$$

where:

$q_c$  – free-field cone resistance interpreted on calibration chamber tests,

$C_0 = 17.68$ ,

$C_1 = 3.10$ .

For a given density index, Eq. (3) can be transformed to Eq. (2).

While a shallow penetration is associated with a surface heave, a deep penetration mechanism is related with the local penetration. A continuous penetration problem is, however, more complex than the study of pile-bearing capacity, as very large soil deformations are induced. During continuous penetration the mini-cones behave more like prototype driven piles, and less like the field CPT (Gui and Bolton 1998). A set of mechanisms of rupture in the form of superimposed slip-line network is proposed (Fig. 5) using the scheme given by Yu and Mitchell (1998) and the works of Sokołowski (1965). An eventual grain size effect during the continuous cone penetration can be related to the soil dilatancy in the shear bands.

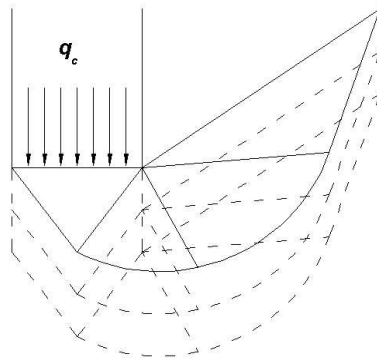


**Fig. 5.** Shear band formation in continuous penetration, modified after Yu and Mitchell (1998)

## 4. Centrifuge Tests

### 4.1. Similitude Conditions

Let us consider a model with dimension  $B$  and the prototype with dimension  $b$ . The scale factor between these two variables can be defined as a geometrical scale  $x^*$ :



$$x^* = \frac{B}{b} = \frac{1}{n}, \quad (4)$$

where:  $n$  – the modelling scale.

The other modelling scales can be defined as:

- stress scale  $\sigma^* = \sigma_M/\sigma_P$ ,
- gravity scale  $g^* = g_M/g_P$ ,
- volumetric density scale  $\rho^* = \rho_M/\rho_P$ ,

where indexes  $M$  and  $P$  denote the model and the prototype, respectively.

The equilibrium condition of continuum mechanics for static loading can be written as:

$$\sum_{j=1}^3 \frac{\partial \sigma_{ij}}{\partial x_j} + \rho \cdot g_i = 0. \quad (5)$$

The dimensional analysis of Eq. (5) needs the following equation to be satisfied:

$$\sigma^* = x^* \cdot g^* \cdot \rho^*. \quad (6)$$

If the same material is used for the model and the prototype ( $\rho^* = 1$ ) and the same stress level is applied ( $\sigma^* = 1$ ) to conserve the soil rheology, and the model  $n$ -times smaller than the prototype is used, the gravity should be  $n$ -times increased to respect the similitude condition (Eq. 6). In this case:

$$g^* = \frac{1}{x^*} = n. \quad (7)$$

The scale factors for centrifuge tests are summarized in Table 1. Time scale factors depend on the phenomena to be studied. Time scale factors for different phenomena and soil-fluid interaction problems are given in (Corté 1989). The principal idea for the physical modelling in centrifuge is given in Fig. 6 for the model size  $B_i$  and gravity scale  $n_i$ .

Three different approaches to the physical modelling in centrifuge can be applied (Fig. 7):

- the study of scale effect with “modelling of models” procedure,
- the size effect analysis,
- the study of stress level effect.

The procedure of “modelling of models” is applied to model a given prototype diameter  $b$  using the cones of different diameter  $B_i$  at different acceleration levels:

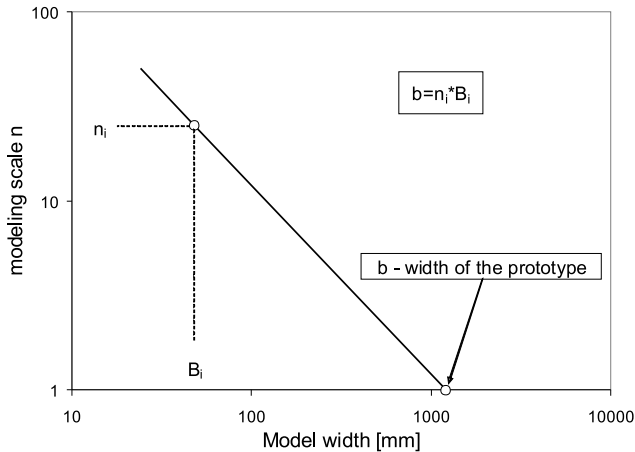
$$b = n_i \cdot B_i = c^{te}, \quad (8)$$

where:  $n_i$  – gravity scale applied for the model  $i$ .



**Table 1.** Scale factors for centrifuge tests

	Prototype	Model
length	1	$n$
surface	1	$n^2$
volume	1	$n^3$
mass	1	$n^3$
time (inertia)	1	$n$
acceleration	1	$1/n$
stress	1	1
strain	1	1
displacement	1	$n$
force	1	$n^2$

**Fig. 6.** Modelling of the prototype

In such a case, the scale effect related to the ratio size of the model  $B_i$  to the mean grain size  $d_{50}$  can be studied for the prototype to be modelled (Fig. 7). When different size prototypes are modelled with a procedure of “modelling of models” (Fig. 8), the size effect can be examined (Fig. 7). In a typical 1 g laboratory tests on different size models, the geometry and particle size effects can be studied. In this case, stress level condition will not be conserved.

In order to study the stress level effect, the same model with a diameter  $B$  is subjected to various acceleration levels (Fig. 7) and the prototypes with different diameters  $b_i$  are modelled:

$$b_i = B \cdot n_i. \quad (9)$$





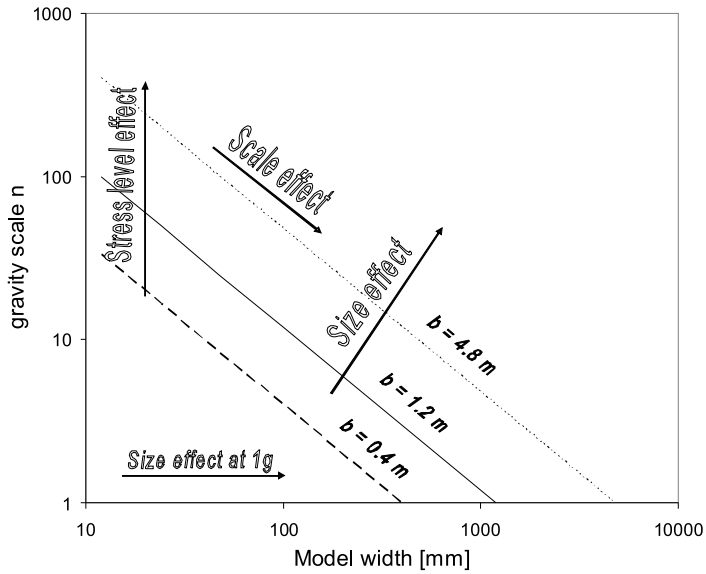


Fig. 7. Definition of scale, size and stress level effects, modified after Ovesen (1979) and Corté (1989)

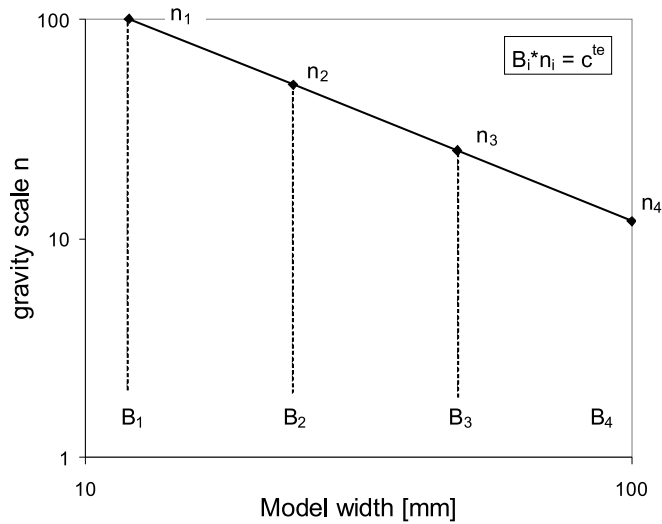
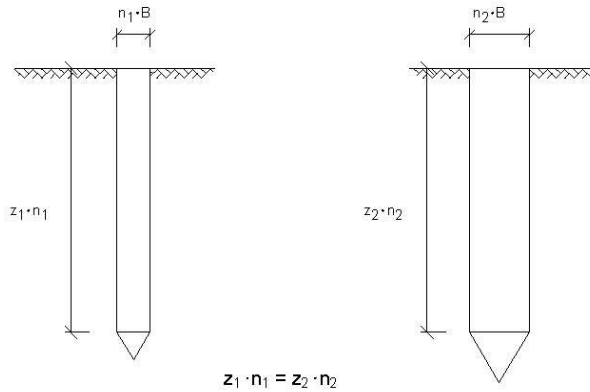


Fig. 8. Modelling of models procedure

#### 4.2. Stress Level Effects in Cone Penetration Tests

When the stress level effect in cone penetration tests is studied in a centrifuge, the different diameter prototypes are modelled (Fig. 9). The interpretation of centrifuge



**Fig. 9.** Prototypes of cones modelled with the stress level effect approach

tests should be made at the prototype scale. At given vertical stress in the prototype scale, different cone penetration to cone diameter ratio is obtained. Different slenderness of the prototypes (Fig. 9) makes a geometry size effect in penetration testing in centrifuge. Moreover, at a given vertical stress in centrifuge, a mini-cone performed at smaller acceleration level could already attain the critical depth, while the same mini-cone subjected to higher acceleration level, i.e. corresponding to the larger prototype diameter, does not reach the critical depth at the same vertical stress, see Fig. 2. It constitutes an additional geometrical distortion in similitude conditions. In the stress level study in centrifuge both grain size and geometry size effects act together, and cannot be properly separated. The grain size effect could be discriminated, only if the procedure of “modelling of models” is applied (Bolton et al 1999).

The objective of this experiment is to verify the existence of size effect in cone penetration testing in centrifuge for small ratio diameter of the model to the mean particle size. This effect consists of grain size and geometry size effect. The tests are executed in two very dense quartz sands of different grain size, where a dilation in the shear bands occurs and a considerable size effect is expected.

### 4.3. Equipment Facility

The tests were executed in the centrifuge of Laboratoire Central des Ponts et Chaussées (L.C.P.C.) in Nantes. The geotechnical centrifuge Model 680 was delivered by Acutronic France SA. The general view of the centrifuge and the possible range of application are given in Fig. 10. The container with the model is placed in the swinging basket. The distance between the rotation axis of the centrifuge and the basket platform is equal to 5.5 m. The basket with 1000 kg mass can rotate at an acceleration of 100 g. The acceleration of 200 g can be applied for the basket mass of 2000 kg.

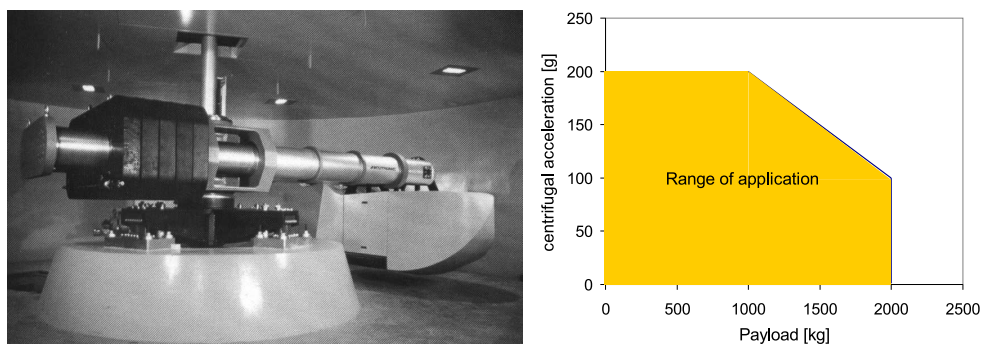


**Fig. 10.** Geotechnical centrifuge and its range of application, L.C.P.C. information

The soil mass is reconstituted with travelling hopper in specially designed pluviation room. The homogeneity of the soil mass was carefully studied with embedded calibration boxes. The systematic controls demonstrate the high level of repeatability of sand raining technique. The sand density variation in the container is less than  $\pm 0.5\%$  and the highest densities are measured close to the walls perpendicular to the direction of the hopper's translation (Garnier 2002).

#### 4.4. Testing Programme

A series of loading tests on model piles of different diameters were performed in the centrifuge of L.C.P.C. in Nantes, to study grain size effect in the shaft friction mobilization. Some additional mini-cone penetration tests were usually performed in the same container. They are used to check the soil mass homogeneity and for comparison with CPT calibration chamber tests performed on the same sand (Bałachowski 1995). The container with inner dimensions  $1200 \times 800 \times 720$  mm was used (Fig. 11). The mechanism of traveling pluviator was automatically adjusted to obtain the density index  $I_D \approx 0.8$ . Two model piles were placed in the container during sand raining in order to model "bored" piles. The prepared container, with mass close to 1900 kg, was transported to the centrifuge chamber and installed in the swinging basket at the centrifuge arm. The mobile penetrometer with remote control was placed on the container. The stroke of the loading piston of the mini-cone is 300 mm.

A typical schedule of the test is given in Fig. 12. The soil mass is conditioned at a given acceleration level ( $n_1 \cdot g$  and  $n_2 \cdot g$ ) and then a pile loading test is performed, followed by a mini-cone penetration test. Unloading-reloading cycles are executed in order to minimize arching and stress concentration in the conditioned soil mass.

In-flight penetration tests at the acceleration  $n_1 \cdot g$  and  $n_2 \cdot g$  were executed in normally consolidated sand mass. Some additional mini-cone tests, not presented in this paper, were also performed in overconsolidated sand, when the acceleration

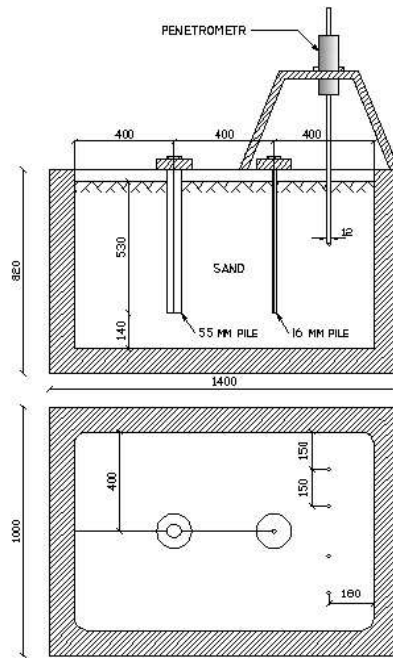


Fig. 11. Container scheme

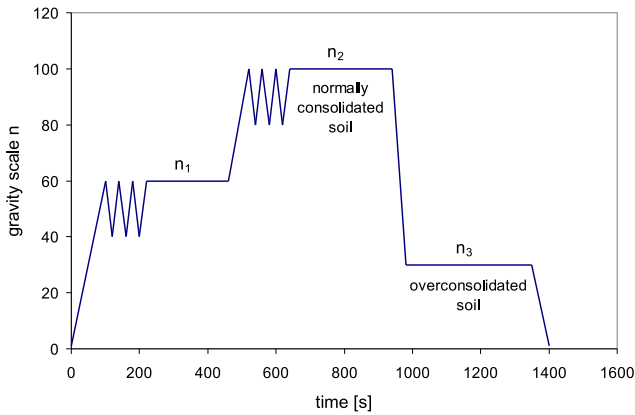


Fig. 12. Typical schedule of centrifuge test

level decreased to  $n_3 \cdot g$ . After the test, the density index from the embedded calibrated boxes was determined (Table 2). The density index higher than the presumed initial one ( $I_D \approx 0.8$ ) can be attributed mainly to the soil conditioning at elevated acceleration levels.

The same mini-CPT model, 12 mm in diameter, was subjected to different acceleration levels ranging from 30 g to 100 g in order to model the prototypes of

different diameter (Table 2). Two uniform ( $U = 1.4$ ) subangular quartz sands with the same mineralogy, but different mean grain diameters, were used:

- medium Hostun sand ( $d_{50} = 0.32$  mm),
- coarse Hostun sand ( $d_{50} = 0.7$  mm).

**Table 2.** Mini-cone tests program

Sand type	$d_{50}$ [mm]	$I_D$	$B/d_{50}$	acceleration
Hostun medium	0.32	0.82	37.5	60 g
				100 g
Hostun coarse	0.7	0.86	17.1	30 g
				60 g
				100 g

The mini-cone tests were performed at a sufficient distance to the model piles and to the container walls to avoid boundary and interference effects (Fig. 11). The analysis of lateral boundary effects, proximity of the container base and the recommendations for performing the CPT in the centrifuge can be found in (Gui et al 1998).

## 5. Test Results

The profile of cone resistance is presented in Figs. 13 and 14 as a function of penetration depth. The tests are stopped when either the maximum stroke of the penetrometer is reached or the risk of the mini-cone damage becomes important, i.e. when the cone resistance exceeded 42 MPa. While rather smooth cone resistance profiles are recorded in medium sand, more irregular profiles are found in coarse sand (Fig. 14).

The results of the centrifuge modelling should be considered in terms of the prototype to be modelled. The profile of the cone resistance is thus presented and compared as a function of vertical effective stress for the prototype (Figs. 15 and 16). While a very similar cone resistance at given vertical stress is found in Hostun medium sand at 60 g and 100 g, some differences are observed for coarse sand, where the cone resistance is systematically higher for the tests executed at lower acceleration level. At higher vertical stress  $q_c$  the profiles tend to converge.

The normalized cone resistance (Eq. (1)) is plotted in Figs. 17 and 18. Two distinct phases in the cone penetration can be distinguished, as was remarked by Gui and Bolton (1998). The first one, before the maximum  $Q$  value is reached, is related to the shallow foundation mechanism. The second one, below the critical normalized depth  $(z/B)_{crit}$ , is governed by a deep foundation scheme and local penetration. Here, the normalized cone resistance decreases with penetration. The penetration mechanism changes from the shallow to the deep foundation at the



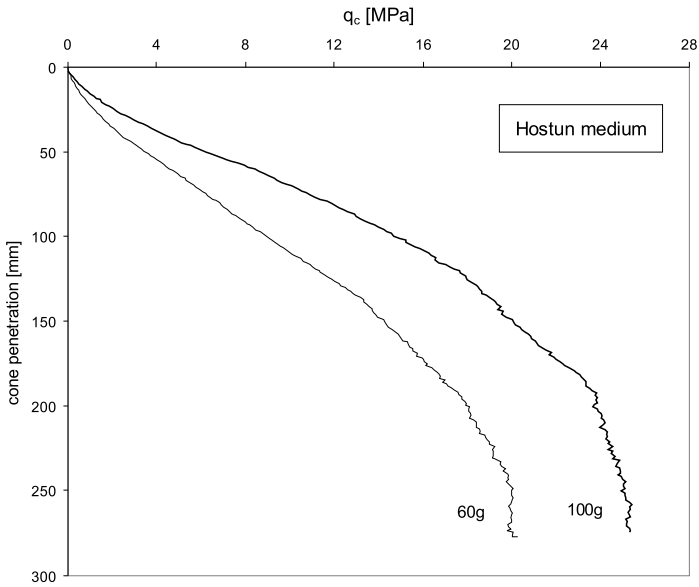


**Fig. 13.** Cone penetration tests in medium sand

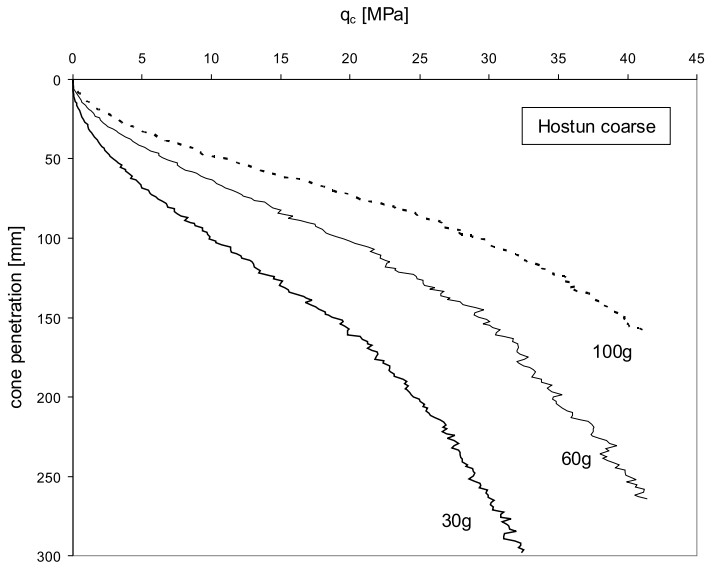


**Fig. 14.** Cone penetration tests in coarse sand

the vertical stress close to 120 kPa in medium sand. In coarse sand this transition depth increases with acceleration level, i.e. with the prototype diameter. While the maximum value of the normalized cone resistance of about 100 is recorded in

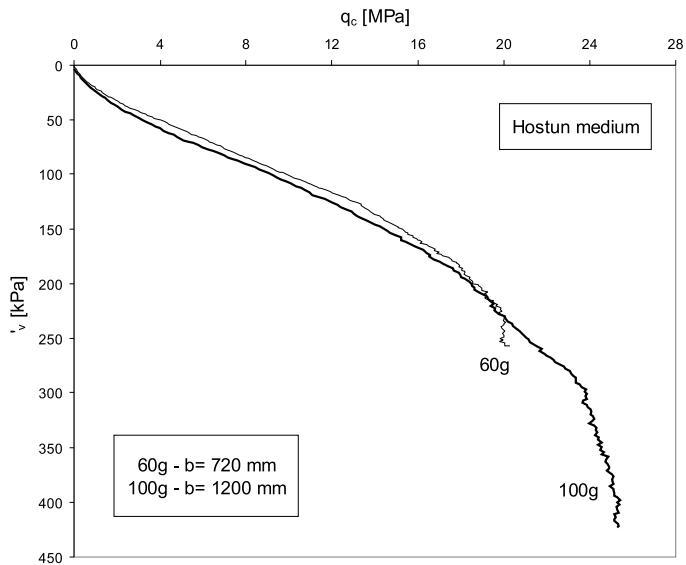


Fig. 15. Set of CPT in centrifuge in medium sand

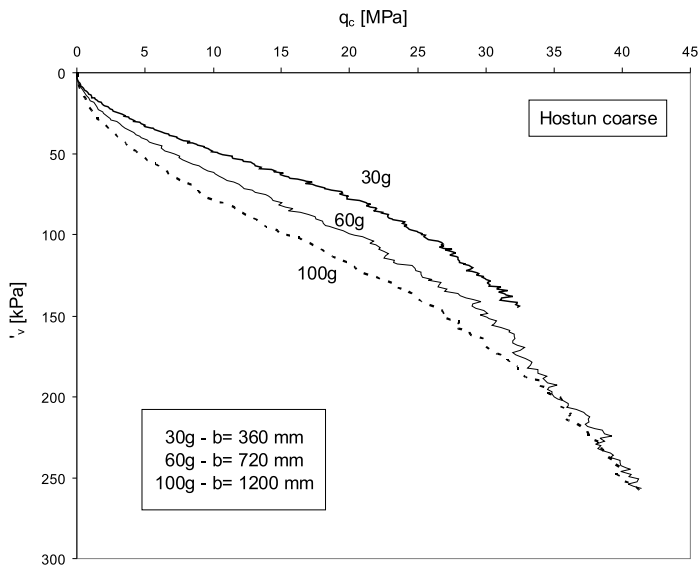
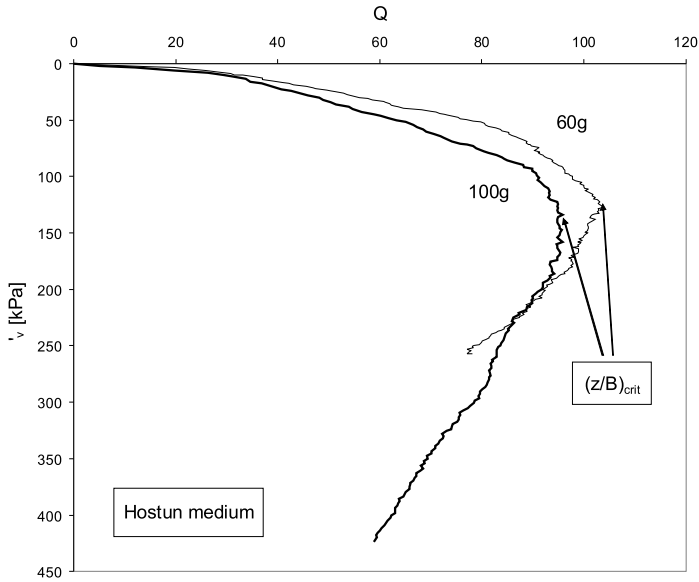
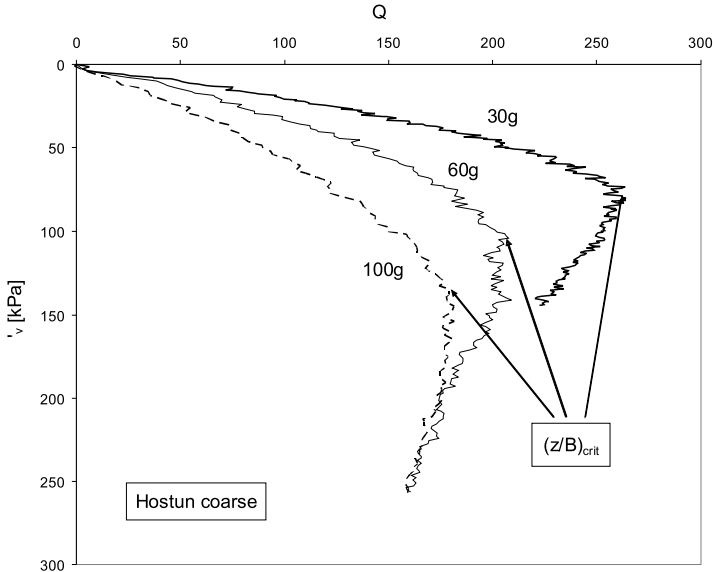


Fig. 16. Set of CPT in centrifuge in coarse sand



**Fig. 17.** Normalized cone resistance in medium sand



**Fig. 18.** Normalized cone resistance in coarse sand

medium sand (Fig. 17),  $Q$  values from 170 to 260 are found in coarse sand (Fig. 18). At a given vertical stress, a higher  $Q$  value is recorded for the prototype with a smaller diameter.





## 6. Discussion

When the idealized model (Fig. 4) is used to interpret the cone penetration tests in the centrifuge, the values of  $k$  close to:

- 40 in medium Hostun sand,
- 80 in coarse Hostun sand are found (Fig. 19).

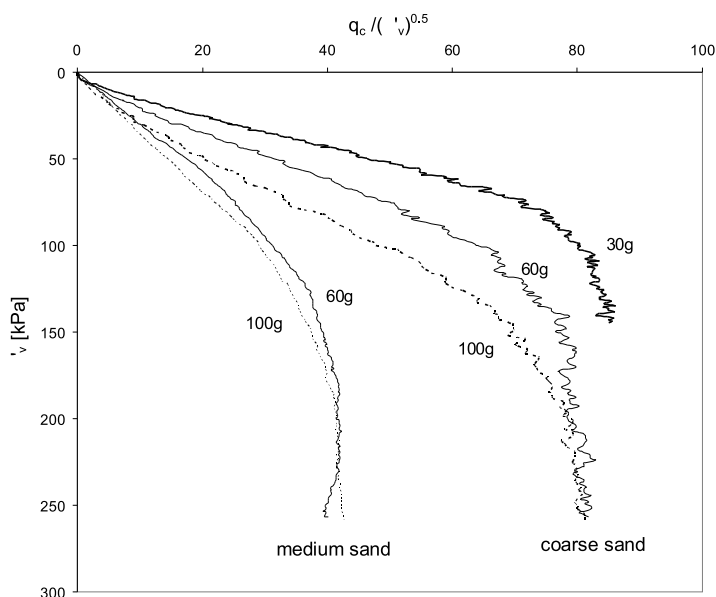


Fig. 19. Normalized cone resistance in both sands vs. vertical stress

A slightly higher  $k$  value found in coarse sand at the end of penetration at 30 g seems to result from the size effect. This effect is reduced at further penetration, with the curve tendency to converge at higher vertical stress.

Let us consider a rigorous approach of “modelling of models”. At given vertical stress the cone penetration to cone diameter ratio ( $z/B$ ) is the same at each acceleration level and no geometrical size effect is present. Since only one size of the mini-cone (12 mm) was used in this series of centrifuge tests, the procedure of “modelling of models” was not executed and the prototypes with different diameters ranging from 360 mm to 1200 mm and different slenderness were modelled. It constitutes a distortion in physical modelling related to the geometry size effect.

In the stress level effect approach used in this study, the particle size and geometry size effects act together and cannot be completely separated. The particle size effect is related to the ratio diameter of the model  $B$  to the mean grain size  $d_{50}$ . This ratio is equal to:



- 37.5 for Hostun medium sand,
- 17.1 for Hostun coarse sand.

The comparison of the cone resistance at 60 g and 100 g in medium sand (Fig. 15) permits the conclusion that no size effect is observed. No particle size effect is noticed in cone penetration tests when  $(B/d_{50})$  ratio exceeds 20, as was found by Bolton et al (1999). As quite similar acceleration levels were applied in the centrifuge modelling in this sand (60 g and 100 g), the cones with similar slenderness were modelled and practically no geometrical size effect was observed. A distinct size effect was found for the tests in coarse sand. The value of the size effects in cone resistance in Hostun coarse sand was estimated in Fig. 20. The assumption was made that no size effect exists for cone penetration test at 100 g, treated as a reference. The size effect at given vertical stress was determined as the ratio of the cone resistance at applied acceleration level to the cone resistance at 100 g. The size effect in coarse sand higher than 2 at 30 g and higher than 1.5 at 60 g was found at low vertical stress. It attenuates with vertical stress and becomes small under the critical depth.

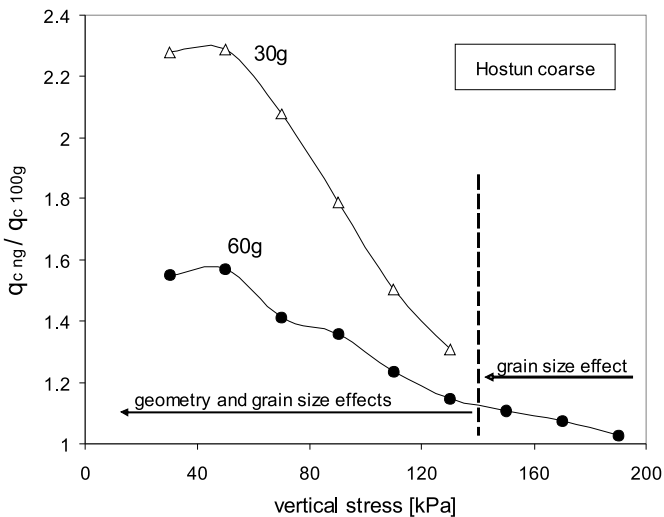


Fig. 20. Size effects in cone resistance in very dense coarse sand

It is difficult to separate the grain size and geometrical size effects. Some grain size effect should be expected in this case ( $B/d_{50} = 17.1$ ), especially at lower vertical stress, where the dilatancy in the sheared zones could be more pronounced. The geometrical size effect is reduced for penetration higher than the critical depth (see Figs. 18 and 19). When normalized to square root of overburden stress, the cone resistance for a given sand reaches very similar values, irrespective of the prototype diameter to be modelled (Fig. 19). It becomes stress level independent. For the



penetration larger than the critical one for the prototype at 100 g, no geometrical size effect is assumed and the difference between the cone resistance at 100 g and 60 g can be attributed to the grain size effect. Approximate discrimination between the grain size effect and the geometry size effect is given in Fig. 20.

The grain size effect in coarse sand is also pronounced in more irregular profiles of the cone resistance (Fig. 16), attributed to crushing and attrition of grains, grain rearrangement and slippage in the cone-grains contact during penetration.

With the same soil used for the model and the prototype, the dilation is not properly scaled in the centrifuge tests. It is higher for the tests on small models in the centrifuge. The use of other material, such as silica flour (Bolton and Lau 1988, de Nicola and Randolph 1999), to meet the similitude conditions, should be executed with caution, after an extensive study of mechanical behaviour of given soil and its fine-grained substitute. Even if a substitute material with the same dilatancy and internal friction angle as for the prototype soil is used, some properties, like crushing strength of grains, could not, however, be fully conserved in the centrifuge modelling (Bolton and Lau 1988).

## 7. Conclusions

A series of mini-cone penetration tests were executed in the centrifuge at different acceleration levels in two very dense Hostun sands to study stress level effect on cone resistance. An additional increase in cone resistance due to particle size and geometry size effects was observed in coarse Hostun sand when the ratio size of the model to the average grain size ( $B/d_{50}$ ) falls to 17.1. At small vertical stress, the cone resistance increased even twice for a small acceleration level. Particle size and geometry size effects attenuate with vertical stress. These size effects act together and could be properly discriminated only if the procedure of “modelling of models” is used. The geometry size effect is reduced at penetration greater than the critical depth. In coarse sand with acceleration level varying from 30 g to 100 g the geometry size effect should be more evident.

No significant size effect was observed in Hostun medium sand at  $B/d_{50} = 37.5$ . Since a relatively narrow range of acceleration (from 60 g to 100 g) was applied in this series of the centrifuge tests, the prototypes with quite similar slenderness are modelled and the geometry size effect was not marked in Hostun medium sand. With the study of stress level some geometrical size effect could appear in this sand if wider acceleration range is applied.

The results of penetration tests should be corrected for the grain size effect if the ratio model diameter to the mean grain size ( $B/d_{50}$ ) falls below 20.

## Acknowledgement

The author appreciates the possibility of conducting experiments with the mini-cone penetration tests in the L.C.P.C. centrifuge in Nantes during his PhD thesis.

## References

- Bałachowski L. (1995) *Différents aspects de la modélisation physique du comportement des pieux: Chambre d'Étalonnage et Centrifugeuse*, Thèse de doctorat, Institut National Polytechnique de Grenoble, France.
- Bałachowski L. (2006) Scale effect in shaft friction from the interface direct shear tests, *Archives of Civil and Mechanical Engineering*, **VI** (3), 13–28.
- Bolton M. D. and Lau C. K. (1988) Scale effects arising from particle size, *Proceedings International Conference Centrifuge'88*, Ed. J. F. Corté, 127–131.
- Bolton M. D., Gui M. W., Garnier J., Corté J. F., Bagge G., Laue J. and Renzi R. (1999) Centrifuge cone penetration tests in sand, *Géotechnique*, **49** (4), 543–552.
- Boulon M. and Foray P. (1986) Physical and numerical simulation of lateral shaft friction along offshore piles in sand, *3<sup>rd</sup> Int. Conference on Numerical Methods in Offshore Piling*, Nantes, 127–147.
- Chow F. C. (1997) *Investigations into the behaviour of displacement piles for offshore structures*, PhD Thesis, University of London (Imperial College), U.K..
- Corté J.-F. (1989) General report/Discussion session 11: Model testing-Geotechnical model tests, *Proceedings of the XII ICSMFE*, Rio de Janeiro, 13–18 August, 2553–2571.
- Dano C., Thorel L. and Rault G. (2005) Interprétation des essais au pressiomètre miniature en centrifugeuse, *Proc. of International Symposium ISP5 – Pressio 2005*, Marne-la-Vallée, Eds. M. Gambin, D. Magnan and Ph. Mestat, **1**, 247–254.
- De Lima D. C. and Tumay M. T. (1991) Scale effects in cone penetration tests, *Geotechnical special publication of ASCE*, Ed. F. G. McLean, No. 27, 38–51.
- De Nicola A. and Randolph M. F. (1999) Centrifuge modelling of pipe piles in sand under axial loads, *Géotechnique*, **49** (3), 295–318.
- Fioravante V. (2002) On the shaft friction modelling of non-displacement piles in sand, *Soils and Foundations*, **42** (2), 23–33.
- Foray P., Bałachowski L. and Rault G. (1998) *Scale effect in shaft friction due to the localisation of deformations*, *Centrifuge'98*, Tokyo, Eds. T. Kimura et al, Balkema, **1**, 211–216.
- Garnier J. (1997) Validation of numerical and physical models: Problem of scale effects, *Proceedings of XIV International Conference on Soil Mechanics and Foundation Engineering*, Hamburg, 659–662.
- Garnier J. (2002) Properties of soil samples used in centrifuge models, *Proceedings Physical modelling in Geotechnics: ICPMG'02*, Ed. R. Philips, P. J. Guo and R. Popescu, Swets and Zeitlinger Lisse, 5–19.
- Garnier J. and König D. (1998) Scale effects in piles and nails loading tests in sands, *Centrifuge'98*, Tokyo, Eds. T. Kimura et al, Balkema, **1**, 205–210.
- Gui M. W. and Bolton M. D. (1998) Geometry and scale effects in CPT and pile design, *Proceedings of International Conference Geotechnical Site Characterization*, Eds. P. Robertson and P. Mayne, Balkema, Rotterdam, 1063–1068.
- Gui M. W., Bolton M. D., Garnier J., Corté J. F., Bagge G., Laue J. and Renzi R. (1998) Guidelines for cone penetration tests in sand, *Centrifuge'98*, Tokyo, Eds. T. Kimura et al, Balkema, **1**, 155–160.
- Habib P. (1985) Effet d'échelle et surface de glissement, *Revue Française de Géotechnique*, (31), 5–10.
- Jamiolkowski M., Ghionna V. N., Lancelotta R. and Pasqualini E. (1988) New correlations of penetration tests for design practice, *Proceedings of the 1st International Symposium on Penetration Testing, (I.S.O.P.T.)*, Orlando, 20–24 March, **1**, 263–296.

- Jamiolkowski M., Lo Presti D. C. F. and Manassero M. (2001) Evaluation of Relative Density and Shear Strength of Sands from CPT and DMT, *Symposia in Honor of C. C. Ladd Soil behaviour and Soft Ground Construction, Geotechnical Special Publications*, No. 119, 5–6 October, Cambridge, Massachusetts, USA.
- Kérisel J. (1962) *Fondations profondes, Annales de l'ITBTP, Série Sols et Fondations*, No. 39, Paris, Novembre 1962.
- Kimura T., Kusakabe O. and Saitoh K. (1985) Geotechnical model tests of bearing capacity problems in a centrifuge, *Géotechnique*, **35** (1), 33–45.
- Kusakabe O., Yamaguchi H. and Morikage A. (1991) Experimental analysis on the scale effect of  $N_y$  for circular and rectangular footings, *Proceedings of the International Conference Centrifuge'91*, Balkema, Rotterdam, 179–186.
- Kutter B. L., Chang J.-D. and Davies B. C. (1994) Collapse of cavities in sand and particle size effects, *Proceedings of International Conference Centrifuge'94*, Eds. C. Leung, F. H. Lee and T. S. Tan, Balkema, Rotterdam, 809–815.
- L.C.P.C. information materials, Nantes.
- Lehane B. M., Gaudin C. and Schneider J. A. (2005) Scale effects on tension capacity for rough piles buried in dense sand, *Géotechnique*, **55** (10), 709–719.
- Lehane B. M. and White D. J. (2005) Lateral stress changes and shaft friction for model displacement piles in sand, *Canadian Geotechnical Journal*, **42** (4), 1039–1052.
- Lunne T., Robertson P. K. and Powel J. J. M. (1997) *Cone Penetration Testing in Geotechnical Practice*, Blackie Academic and Professional.
- Ovesen N. K. (1979) The scaling law relationship, *Panel discussion, Proc. 7<sup>th</sup> European Conf. on Soil Mech. and Found. Eng.*, Brighton, **4**, 319–323.
- Reddy E. S., Chapman D. N. and Sastry V. V. R. N. (2000) Direct shear interface test for shaft capacity of piles in sand, *Geotechnical Testing Journal*, **23** (2), 199–205.
- Sokołowski V. V. (1965) *Statics of Granular Media*, Pergamon Press, Inc., Tarrytown, N.Y.
- Stone K. J. L. and Wood M. (1992) Effects of dilatancy and particle size observed in model tests on sand, *Soils and Foundations*, **32** (4), 43–57.
- Tatsuoka F., Okahara M., Tanaka T., Tani K., Morimoto T. and Siddiquee M. (1991) Progressive failure and particle size effect in bearing capacity of a footing on sand, *Geotechnical Engineering Congress, Geotechnical Special Publication of ASCE*, No. 27, 788–802.
- Wernick E. (1977) Stresses and strains on the surface of anchors, *IX. ICSMFE*, Tokyo, Special Session 4, 113–119.
- White R. J., Stone K. J. L. and Jewell R. J. (1994) Effect of particle size on localisation development in model tests on sand, *Proceedings of International Conference Centrifuge'94*, Eds. C. Leung, F. H. Lee and T. S. Tan (eds), Balkema, Rotterdam, 817–822.
- Yu H. S. and Mitchell J. K. (1998) Analysis of cone resistance: review of methods, *Journal of Geotechnical and Geoenvironmental Engineering*, **124** (2), 140–149.

